First-principles formation energies of monovacancies in bcc transition metals

Per Söderlind, L. H. Yang, and John A. Moriarty
Physics Directorate, Lawrence Livermore National Laboratory, University of California, P.O. Box 808, Livermore, California 94551

J. M. Wills
Theoretical Division, Los Alamos National Laboratory, Los Alamos, New Mexico 87544
(Received 12 July 1999; revised manuscript received 20 October 1999)

Monovacancies for seven bcc *d*-transition metals V, Cr, Fe, Nb, Mo, Ta, and W have been studied in detail from first-principles calculations. A full-potential, linear muffin-tin-orbital (FP-LMTO) method has been used in conjunction with both the local-density approximation (LDA) and the generalized-gradient approximation (GGA) to calculate volume-relaxed vacancy formation energies in all seven metals. A complementary *ab initio* pseudopotential (PP) method has been used to calculate both volume- and structure-relaxed LDA formation energies and formation volumes in V, Nb, Mo, Ta, and W. Fully relaxed PP geometries have also been applied to FP-LMTO LDA and GGA calculations. From these results, the following clear trends and conclusions emerge: (i) for the same fully relaxed geometry, FP-LMTO-LDA and PP-LDA formation energies are nearly identical; (ii) the lowest calculated formation energies are within or close to experimental error bars for all bcc metals except Cr, and the overall agreement with experiment is better for the $4d$ and $5d$ metals than the $3d$ metals; (iii) GGA and LDA formation energies are very similar for the $4d$ and $5d$ metals but for the $3d$ metals, and especially Fe, GGA performs better; (iv) volume- and structural-relaxation contributions lower the calculated formation energy by 0.1–0.5 eV, and improve agreement with experiment; (v) fully relaxed LDA formation volumes are in the narrow range $(0.45–0.62)\Omega_0$, where Ω_0 is the equilibrium atomic volume; and (vi) the dominant structural effects are an approximate 5% inward relaxation of the first near-neighbor shell for group-V metals and a corresponding 1% inward relaxation for group-VI metals, with the exception of Mo, for which the second-shell atoms also relax inward by about 1%.

I. INTRODUCTION

During the last decade, computational techniques and resources have developed to a degree that now allow for detailed first-principles studies of important defect properties in both simple and *d*-transition metals, including vacancies, interstitials, and grain boundaries. This advance is important because it could help bridge the gap between phenomenological descriptions of macroscopic mechanical properties and microscopic theories seeking to elaborate and link the different length scales determining these properties. For example, one can use basic ground-state and defect properties for a material, calculated from first-principles electronic-structure techniques, to help develop quantum-based interatomic potentials that can be applied to the study of extended defects and defect-defect interactions involving many thousands or tens of thousands of atoms. These results in turn can provide fundamental input into mesoscale and macroscale simulations of mechanical properties for the material under consideration. This is an *ab initio* multiscale modeling approach for which the ultimate goal is to understand and predict the macroscopic behavior of a material, under a wide variety of conditions, without relying upon any phenomenological assumptions or input. We are currently developing such an approach to treat plasticity and strength in bcc transition metals,[1] with tantalum (Ta) as the prototype material. First-principles density-functional calculations of structural, elastic, vibrational, and mechanical properties have been carried out on Ta over a wide pressure range.[2] These results have enabled the construction of accurate many-body interatomic potentials, which in turn are being used to study point and extended defects in Ta, including the structure and energetics of dislocations. One important input quantity in this regard is the vacancy formation energy (E^f_{vac}), which determines the vacancy concentration at finite temperature and contributes to self-diffusion and dislocation climb in the metal. Realistic interatomic potentials for multiscale modeling should be able to produce accurate monovacancies, so a first-principles understanding of vacancy formation is highly desirable.

The importance of *ab initio* studies on the formation of monovacancies was acknowledged early on, and the first such calculations, based on density-functional theory[3,4] in the local-density approximation (LDA), were done for simple metals almost two decades ago.[5] In the early 1990s, *d*-transition metals also began to be studied with LDA methods.[6] For metals with narrow *d* bands, and especially $3d$ bands, vacancy calculations were a challenge for pseudopotential (PP) techniques and therefore other, more time consuming, all-electron methods have been utilized for this purpose. In this regard, Korhonen *et al.*[7] used a full-potential, linear-muffin-tin-orbital (FP-LMTO) method to calculate monovacancies for six bcc and six fcc *d*-transition metals with mixed success. Also, more recently, Korzhavyi *et al.*[8] used a more approximate order-*N* Green's-function method to calculate E^f_{vac} for all of the *d*-transition and nobel metals. Generally speaking, for the fcc metals these all-electron results are in reasonable agreement with each other and with experimental data, although the vacancy formation energies of Korhonen *et al.* tend to be somewhat larger and in better

agreement with experiment than those of Korzhavyi *et al.* Conversely, for most bcc metals there are substantial discrepancies between these two methods and the overall agreement with experiment is considerably poorer. The difference between the E^f_{vac} results of Korhonen *et al.* and Korzhavyi *et al.* is in fact sufficiently large (0.4–1.1 eV) that we will focus mostly on the former, more closely related FP-LMTO results in the discussion below.

The fcc FP-LMTO results of Korhonen *et al.*[7] have also confirmed previous calculations,[9] while for the bcc metals there have been fewer published calculations with which to compare. However, subsequent work on bcc Mo using a mixed-basis pseudopotential method[10] as well as independent FP-LMTO calculations[11] do provide support for the result of Korhonen *et al.* for that metal.

In the PP work, the agreement with experiment was improved by allowing for volume and structural relaxations in the calculations, although even without those refinements the result for Mo is already in good agreement with experiment and the (unrelaxed) FP-LMTO calculations.[7,11] Instead, the largest discrepancies between the calculations of Korhonen *et al.* and experiment were for V, Cr, and Ta. Recently fully relaxed PP calculations for Ta (Ref. 12) and *W* (Ref. 13) gave, however, better results compared to experiment. For W a recent unrelaxed FP-LMTO result[11] was also in better agreement with experiment.

In light of the importance of monovacancies in the understanding of materials properties and the large disagreements between first-principles theory and experiment for some of the bcc *d*-transition metals, we have chosen to study all seven bcc *d*-transition metals, including iron, in the present work using both FP-LMTO and *ab initio* PP methods. To examine the effects of the exchange and correlation treatment on the calculated vacancy formation energy, we have employed the generalized-gradient approximation (GGA) in addition to the standard LDA for the electron exchange-correlation functional. Furthermore, unlike Korhonen *et al.*,[7] we do allow volume and structural relaxation in our calculations. To include structural relaxation in our all-electron results, we use a unique combination of FP-LMTO and PP calculations, which capitalizes on the strengths of both methods.

Our paper is organized as follows. Section II deals with computational details of the two electronic structure methods used in the work, namely, the FP-LMTO and *ab initio* PP methods. Section III treats numerical convergence issues, equilibrium volumes, and bulk moduli, and finally vacancy formation energies and volumes for seven bcc *d*-transitions metals. We conclude and summarize in Sec. IV.

II. COMPUTATIONAL APPROACH

A. FP-LMTO method

Our FP-LMTO calculations are done within the framework of density-functional theory using state-of-the-art approximations to the electron exchange-correlation effects. In practice, we are solving the one-electron Kohn-Sham equations[4] self-consistently for a periodic system. For the exchange-correlation potential we have employed both the robust local-density approximation, as parametrized by von Barth and Hedin,[14] and also a more accurate approximation that includes ''nonlocal'' information about the electron density by means of gradient correction terms to the electron density, the generalized-gradient approximation.[15] The periodicity of the system was ensured by the standard supercell, for which we used either a 27-, 54-, or 128-atom cell size. Most of our calculations were done for the 27-atom supercell. The one-electron Schrödinger equation was solved for an effective Hamiltonian that included scalar relativistic terms but not spin-orbit coupling.

The specific technique we employ is one of several commonly used variants of the full-potential, linear muffin-tin orbital method and originates with Wills and co-workers.[16] In our calculations, the one-electron wave functions were comprised of so-called muffin-tin-orbital basis functions that were expanded to include $4s$, $4p$, and $3d$ for V, Cr, and Fe; $5s$, $5p$, and $4d$ for Nb and Mo; and $6s$, $6p$, and $5d$ for Ta and W. Although this approach produced sufficiently converged results for the LDA treatment, as test calculations for V, Mo, and Ta with extended semi-core states showed, well-converged GGA calculations required the use of these latter semi-core states. Hence for the GGA calculations we used basis sets of $3s3p+4s4p3d$ for the $3d$ metals, $4s4p+5s5p4d$ for the $4d$ metals and $5s5p+6s6p5d5f$ for the $5d$ metals. An exception to this was the 54-atom supercell calculation for Mo, for which we retained a minimal basis set. In each case, the core-electron density was obtained by solving the relativistic Dirac equation self-consistently.

The use of the full nonsphericity of the charge density is essential for accurate total energies in open structures such as a bcc lattice with a vacancy. This is accomplished in our method by expanding the charge density and potential in cubic harmonics inside nonoverlapping muffin-tin spheres and in a Fourier series in the interstitial region. The size of the muffin tins was chosen such that they filled about 60% of the total volume (i.e., a 40% interstitial region). Spherical harmonic expansions were carried out through $l_{max}=6$ for the bases, potential, and charge density.

For Cr and Fe we also allowed for a spontaneous magnetic moment to form. In Cr this treatment lowered the total energy somewhat, but gave essentially the same vacancy formation energy as a paramagnetic treatment. For Fe, on the other hand, the magnetic interactions are very important and had a great impact upon the calculated E^f_{vac}.

The convergence of the vacancy formation energy with respect to number of *k* points used in the Brillouin-zone sampling was investigated for most of the metals in the study. The number of *k* points needed to converge the result is of course dependent upon the actual cell size. For a larger supercell a smaller number could be used because of the smaller volume of the Brillouin zone. For the 27-atom supercell we typically used sets of 14 and 40 *k* points.

B. Plane-wave pseudopotential model

For V, Nb, Mo, Ta, and W we also used an *ab initio* pseudopotential method to calculate the fully relaxed configurations of supercells both with and without a vacancy present. The PP calculations were done within the framework of density-functional theory but only in the LDA and with the Ceperley-Alder[17] electron exchange-correlation functional, as parametrized by Perdew and Zunger.[18] The

pseudopotentials used in the present work are nonlocal and norm conserving, and were constructed in a manner similar to that previously described for Ta.[18] In particular, the Ta pseudopotential was successfully applied[19] to calculate accurate surface properties as well as phonons. The PP method is implemented in a plane-wave basis set, with a cutoff used here of 40 Ry for Ta and W, 50 Ry for Mo, and 60 Ry for V and Nb.

One of the major strengths of the PP methods is that full relaxation of the supercell, both with respect to volume and structure, is readily accommodated. In the PP method, for a given structure the positions of ions were determined by minimizing the residual vectors defined by the Hellmann-Feynman forces on the ions using a quasi-Newton method.[20] The unit-cell parameters were then determined by making adjustments using the quasi-Newton method until the stress tensor[21] was within a set tolerance. The structural parameters were considered to be fully relaxed when the forces on the ions were less than 0.02 eV/Å and all stress tensor components were less than 1 kbar. In the FP-LMTO method, on the other hand, only volume relaxation is directly accommodated. To calculate the effect of structural relaxation in V, Mo, Nb, W, and Ta with this method, we have used the final relaxed PP ion configurations back in additional FP-LMTO LDA and GGA calculations. This procedure is internally consistent in that for the same fully relaxed ion configurations PP-LDA and FP-LMTO-LDA calculated formation energies are found to be nearly identical. Thus we also refer to FP-LMTO results so obtained as fully relaxed.

C. Vacancy formation energy and formation volume

In the calculations of the vacancy formation energy, we compare the total energy for a supercell with N atoms and no vacancy $[E_{tot}(N,\Omega_N)]$ and the total energy for a supercell with $N-1$ atoms and one vacancy, placed in the center, $[E_{tot}(N-1,\Omega_{N-1})]$. This procedure maximizes the cancellation of numerical errors in the calculation of E^f_{vac}, which is computed as

$$E^f_{vac}=E_{tot}(N-1,\Omega_{N-1})-\frac{N-1}{N}E_{tot}(N,\Omega_N). \qquad (1)$$

Here Ω_{N-1} and Ω_N are the respective relaxed supercell volumes, such that

$$\Omega_N=N\Omega_0, \qquad (2)$$

where Ω_0 is the bulk equilibrium atomic volume. The energy bands in the calculation of E^f_{vac} were calculated for 14–40 k points (27 atoms/cell) or 10–35 k points (54 atoms/cell) using the special k-point method. For the largest supercell considered (128 atoms/cell), the results were well converged for four k points. In addition to this, we further improved convergence through a Gaussian broadening procedure in which we associated with each eigenvalue used in the calculations a Gaussian having a width of 0.2–0.3 eV.

It is also of interest to calculate the corresponding vacancy formation volume Ω^f_{vac}. This is defined as the volume difference between the volume gained by rigidly removing one atom from the bulk, Ω_0, and the volume lost when the vacancy is fully relaxed in the supercell, $\Omega_N-\Omega_{N-1}$:

TABLE I. Absolute (eV) and relative difference between unrelaxed FL-LMTO calculations of bcc monovacancies using a 27- and 54-atom supercell size.

Metal	$E^{54}_{vac}-E^{27}_{vac}$	$E^{54}_{vac}-E^{27}_{vac}/E^{54}_{vac}$
V	−0.14	−6.0%
Cr	0.06	2.6%
Nb	−0.22	−7.6%
Mo	0.40	12%
Ta	0.20	5.4%
W	0.19	5.1%

$$\Omega^f_{vac}=\Omega_0-(\Omega_N-\Omega_{N-1}). \qquad (3)$$

In the present investigation we chose the 27-atom supercell to calculate the formation volume. Test calculations on 54-atom supercells indicated that those were converged to the 10% level for the formation volumes.

III. RESULTS AND DISCUSSION

A. Numerical convergence

Before presenting the results of our calculations for the vacancy formation energies, we discuss possible errors due to numerical approximations in our computations. The convergence as a function of supercell size, Brillouin-zone sampling (k points), and basis-set size need to be ensured. Below we show the results of those convergence tests. They were all done in the same manner and based on FP-LMTO calculations. The volumes of the supercells, both with and without the vacancy, were chosen to correspond to the bulk experimental density. In other words, Ω_N/N and $\Omega_{N-1}/(N-1)$ were set equal to the experimental atomic volume Ω_0 at ambient pressure. This procedure may not be conventional for a fixed supercell calculation, and it is perhaps more common to choose a fixed supercell *volume* rather than a fixed *atomic density*. But these two procedures will, of course, converge at large enough N. Also, all the convergence tests reported below were done using the LDA treatment of exchange and correlation[14] rather than the GGA treatment.[15]

Let us first discuss the effect of the supercell size. For defects in metals, it has been shown that already quite small supercells may give well-converged results. In our calculations we used 27-, 54-, and 128-atom supercells in investigating this issue. For V, Cr, Nb, Mo, Ta, and W we compared results for E^f_{vac} calculated at the experimental density with 27- and 54-atom supercells. The differences, in relative and absolute numbers, are shown in Table I. Notice that for most metals the difference is of the order of 5%, which, in light of other approximations we have introduced, may be considered as relatively well converged. For Mo, however, the difference is rather high, 12%. For this reason we decided to do structure- and volume-relaxed calculations for Mo using the 54-atom supercell, whereas for the others we used the 27-atom supercell. The volume-relaxed LDA result for Mo, using the 27-atom supercell, was 2.88 eV. This is somewhat smaller than the unrelaxed result of 3.13 eV reported by Korhonen *et al.*[7] for the same supercell size. In an attempt to compare with their results, we also calculated the E^f_{vac} for a fixed 27-atom supercell volume (lattice constant 17.80 a.u.),

TABLE II. Absolute (eV) and relative difference between unrelaxed FP-LMTO calculations of bcc monovacancies using 14 and 40 k points for the 27-atom supercell size.

Metal	$E^{27}_{vac}(40)-E^{27}_{vac}(14)$	$E^{27}_{vac}(40)-E^{27}_{vac}(14)/E^{27}_{vac}(40)$
V	0.05	2.0%
Cr	−0.05	−1.5%
Nb	0.00	0.0%
Mo	0.08	2.9%
Ta	−0.11	−3.8%
W	0.03	1.0%

and our result was then closer to theirs, 3.06 eV. We also used Ceperley-Alder exchange correlation[17] instead of the von Barth and Hedin parametrization,[14] but the result was insensitive (less than 1% difference) to the actual choice. The vacancy formation energy for Mo increases considerably when our calculations are performed for a 54-atom supercell (as expected from our convergence tests), yielding 3.39 eV, so that the difference is about 0.5 eV. This conclusion is in disagreement with that of Meyer and Fähnle,[10] who claimed convergence to within about 0.15 eV for the 27-atom supercell. For the volume-relaxed case, their 54-atom supercell vacancy formation energy was close to 3.0 eV. Allowing the structure relaxation decreased this value only slightly to 2.90 eV in their pseudopotential treatment, a result which is confirmed in our PP calculations. Our fully relaxed FP-LMTO result, on the other hand, showed a drop of about 0.4 eV form the volume-relaxed value, with a final value much closer to Meyer and Fähnle, 3.0 eV.

The number of k points necessary to converge the Brillouin-zone integration is of course dependent upon the supercell size. Fewer k points are necessary in a larger supercell to maintain the same k-point density in reciprocal space. Because most of our calculations have been made for a 27-atom supercell, we studied the k-point convergence most carefully for this case. Table II shows the absolute and relative difference between the E^f_{vac} calculated with 14 and 40 k points. The average absolute difference is of the order of 0.05 eV, with the worst case being Ta (0.11 eV). In relative numbers, the difference is about 2% on average between the 14- and 40-k-point calculations. In comparison to other approximations we have made in the calculations, we consider the 14-k-point calculation being well converged and we have therefore chosen to focus on calculating the vacancy formation energy for all metals, except Mo, using 14 k points and a 27-atom supercell geometry. For Mo we instead used ten k points and a 54-atom supercell geometry.

The effect of basis-set size upon the monovacancy formation has been investigated for three of the studied metals, V, Mo, and Ta. It was previously argued that using a standard minimal basis set, with two kinetic-energy parameters, would cause the vacancy formation energy to be too large in general.[13] This was not found to be the case for our LDA calculations, however. In V, Mo, and Ta, we increased the size of the basis set considerably to check the numerical convergence of our minimal basis-set treatment. The price one has to pay for this increase in accuracy is of course an increase in computational burden, where we had to diagonalize a matrix of more than double the dimension (40 instead of 18 per atom) and the computational time increases cubically with this dimension increase. In Table III we show our results from this convergence test. In all three cases considered, the extended basis set results in a higher vacancy formation energy, but the increase is almost negligible. The difference in each case amounts to less than 0.15 eV, and, again, considering other approximations made, this is satisfactory convergence for our purposes. This conclusion, however, is in disagreement with the calculation by Korzhavyi *et al.*[8] In their calculation, excluding the f orbital from the basis set increased their E^f_{vac} for Mo on the order of 30%. This effect seems to us to be severely overestimated in their approach, and may explain the large discrepancies with FP-LMTO calculations[7] their method produced for most of the bcc d-transition metals.

TABLE III. Absolute (eV) and relative difference between unrelaxed FP-LMTO calculations of bcc monovacancies using a minimal and extended basis set.

Metal	$E^{sp+spdf}_{vac}-E^{spd}_{vac}$	$E^{sp+spdf}_{vac}-E^{spd}_{vac}/E^{sp+spdf}_{vac}$
V	0.14	3.4%
Mo	0.04	1.0%
Ta	0.08	2.1%

The minimal basis-set treatment, in conjunction with the GGA gave, however, a very large vacancy formation energy for Ta (about 0.5 eV too large). For this reason we used an extended basis for all GGA calculations except for the 54-atom supercell treatment for Mo. We believe this is reasonable because for Nb (the neighboring d metal) the difference in E^f_{vac} between the minimal basis-set calculation and the extended basis-set calculation was found to be negligible (<0.05 eV).

B. Bulk results

Before discussing the remaining results connected to the formation of a vacancy in the metal, we first present and discuss our results for the equilibrium volume and bulk modulus obtained for the supercell without a vacancy present. Table IV shows calculated atomic equilibrium volumes (Ω_{th}) and calculated bulk moduli, evaluated at both the theoretical equilibrium volume (B^{th}) and experimental equilibrium volume (B^{th}_0), together with experimental data (Ω_0 and B_0). For comparison, the FP- LMTO-LDA and FP-LMTO-GGA calculations were done here with the same, smaller, basis set. Notice that the FP-LMTO-GGA approach generally gives the best equilibrium volume and bulk modulus compared to experiment. The largest discrepancies are found for V and Cr. For Cr, the results could be improved somewhat by allowing for ferromagnetic order in the calculations, but this was not done here because it had little effect upon the vacancy formation energy, as discussed above. Vanadium, on the other hand, is nonmagnetic and the discrepancy between theory and experiment is larger than one would expect. Obviously, the GGA is an improvement over the LDA, but still there seems to be a need for a better treatment of the electron exchange and correlation effects in this metal. In comparing the FP-LMTO-LDA and PP-LDA results, one sees some small differences, which may be of

TABLE IV. Calculated and experimental equilibrium volumes (Å^3) and bulk moduli (GPa) for the seven bcc *d*-transition metals.

	FP-LMTO-LDA			FP-LMTO-GGA			PP-LDA			Expt.[a,b]	
Metal	Ω^{th}	B^{th}	B_0^{th}	Ω^{th}	B^{th}	B_0^{th}	Ω^{th}	B^{th}	B_0^{th}	Ω_0	B_0
V	12.6	202	148	13.3	152	134	12.9	230	155	13.9	157
Cr	10.9	291	199	11.5	244	205				12.0	190
Fe	10.5	246	158	11.4	195	169				11.7	173
Nb	17.2	177	151	18.2	152	157	17.1	192	164	18.0	173
Mo	15.2	277	254	15.7	252	266	15.2	283	256	15.5	265
Ta	17.3	202	180	18.1	172	183	17.1	220	183	17.9	194
W	15.6	319	295	16.2	284	310	15.3	317	287	15.9	314

[a]Donohue (Ref. 31).
[b]Kittel (Ref. 32).

some importance for the vacancy formation energies obtained from the two methods. In particular, the two methods are in greatest disagreement for the equilibrium volumes of V and W, where the FP-LMTO-LDA approach yields a 0.3 Å^3 larger volume per atom than the PP-LDA approach. Consequently, V and W are the two metals where one would expect the largest difference between FP-LMTO-LDA and PP-LDA vacancy formation energies.

C. Volume relaxation

In the previous FP-LMTO study by Korhonen *et al.*,[7] the formation energy was calculated for a fixed supercell volume. Here we improve upon their approach by allowing the supercell to relax to its optimum volume. This was accomplished by calculating the total energy for five volumes and then numerically fitting the energies to a Murnaghan equation of state.[22] In addition to the increased accuracy allowed by this procedure, one does not need to artificially specify a lattice parameter (supercell volume) at which the calculations are performed. In Fig. 1 we show the effect of volume relaxation for a 27-atom LDA supercell calculation of E_{vac}^f for Ta. Here the unrelaxed 26-atom total energy of Ta with and without a vacancy is shown as a function of atomic volume. At the experimental atomic volume (~18 Å^3) E_{vac}^f is about 3.1 eV. The volume-relaxed E_{vac}^f, however, is close to 3.6 eV. Our volume-relaxed FP-LMTO-LDA results for

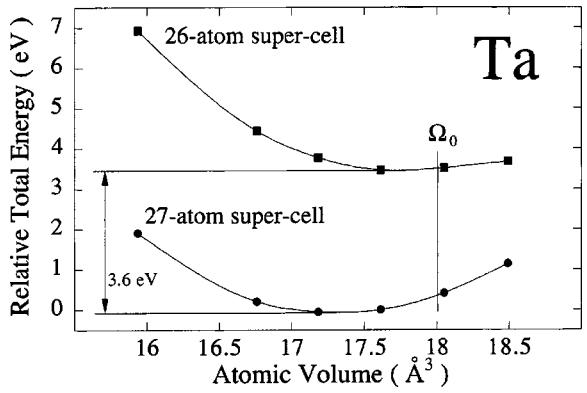

FIG. 1. FP-LMTO-LDA 26-atom total energies for Ta with (26 atoms) and without (27 atoms) a vacancy but no structural relaxation. At the experimental atomic volume (18 Å^3) E_{vac}^f is about 3.13 eV, while the volume-relaxed of E_{vac}^f is about 3.6 eV.

all seven bcc metals area given in Table V together with previously published theory[7,8,10–13] and experimental data.[23–27] In addition to our LDA results, we also present our volume-relaxed GGA results in the fourth column of Table V. Note that for all seven metals the volume-relaxed LDA and GGA results are rather close (within ~0.2 eV). It was previously speculated that a GGA treatment, compared to a LDA treatment, would significantly lower the formation energy in Cr and V, but our calculations instead show that the change in E_{vac}^f is only about 0.2 eV or less in both cases.

When fully relaxed, only Fe shows a substantially lower vacancy formation energy with the GGA. To clarify the role of magnetism in this metal, we performed nonmagnetic FP-LMTO-GGA calculations, and found that the volume-relaxed formation energy drops to 1.4 eV, considerably lower than the corresponding magnetic result, 2.60 eV. These results are qualitatively consistent with the experimental data of De Schepper *et al.*,[26] who found that the vacancy formation energy in iron was lower in the paramagnetic state (1.79 eV) compared to the ferromagnetic state (2.0 eV). We conclude that magnetic effects are indeed important for monovacancy formation in bcc Fe.

D. Structural relaxation

For V, Nb, Mo, Ta, and W, we used *ab initio* pseudopotential LDA calculations to perform both volume and structural relaxations around the vacancy. The fully relaxed values of E_{vac}^f obtained from these calculations are shown in Table V in the column labeled ''PP-LDA.'' Overall, these results agree rather well with the experimental observed data, although the theoretical values for V and W are, respectively, about 0.3 eV above and below the error bars of the data. From the fully relaxed PP-LDA calculations one can also extract the formation volume Ω_{vac}^f from Eq. (3). For a comparison we also show the formation volumes obtained from volume-relaxed-only calculations in Table V. In the case of Mo, we note that our fully relaxed result, 0.50 Ω_0 in Table V, is in exact agreement with that of Meyer and Fähnle.[10] Although we did consider second- and third-nearest-neighbor shells in the relaxation for the 27- and 54-atom supercells, respectively, we found that the first-nearest-neighbor shell dominates the relaxation energies. We also noticed that the first shell relaxed inward in a similar fashion for V, Nb, and Ta. The inward relaxation is on the order of

TABLE V. Vacancy formation energies E^f_{vac} (in eV) for the seven bcc *d*-transition metals. All of the present FP-LMTO and PP results were obtained from 27-atom supercell calculations, using 14 *k* points, except for Mo where a 54-atom supercell (ten *k* points) calculation was performed. A 54-atom supercell was also used for Ta but this gave almost the same LDA result, $E^f_{vac}=3.10$ eV (both FP-LMTO-LDA and PP-LDA). The volume-relaxed (vol rel) FP-LMTO and the fully relaxed (full rel) PP results are from internally self-consistent calculations. The fully relaxed FP-LMTO results are for the corresponding PP configurations, except for Cr and Fe. For Cr and Fe, the relaxed PP configurations of W and Ta were used, respectively, as described in the text. The vacancy formation volume Ω^f_{vac}, in units of the equilibrium atomic volume Ω_0, was calculated with the PP-LDA approach.

	FP-LMTO-LDA		FP-LMTO-GGA		PP-LDA	Published theory[a]	Expt.[b]	Ω^f_{vac}	
Metal	vol rel	full rel	vol rel	full rel	full rel			vol rel	full rel
V	3.07	2.65	3.28	2.55	2.48	3.06	2.1–2.2	0.37	0.52
Cr	3.06	(3.02)	2.87	(2.85)		2.86	2.0–2.4		
Fe	2.76	(2.68)	(2.60)	(2.18)		2.25[c]	1.8–2.2		
Nb	3.10	2.79	3.14	2.88	2.82	2.90	2.6–3.0	0.30	0.45
Mo	3.39	3.00	3.30	2.90	2.85	3.13,2.90[d],3.14[e]	2.6–3.2	0.45	0.50
Ta	3.60	3.20	3.74	3.20	3.20	3.49,3.00[f]	2.8–3.1	0.47	0.60
W	3.69	3.64	3.63	3.60	3.35	3.27,3.53[e],3.77[g]	3.5–4.1	0.55	0.62

[a]Unrelaxed FP-LMTO results; Korhonen *et al.* (Ref. 7) except as noted.
[b]Experimental results; H. Schultz and P. Ehrhart (Ref. 23), H.-E. Schaefer (Ref. 24), Fürderer *et al.* (Ref. 25), De Schepper *et al.* (Ref. 26), R. Zeigel and H.-E. Schaefer (Ref. 27), and J. N. Mundy (Ref. 33).
[c]Volume-relaxed Green's-function LMTO result; Korzhavyi *et al.* (Ref. 8).
[d]Fully relaxed mixed-basis PP result; B. Meyer and M. Fähanle (Ref. 10).
[e]Unrelaxed FP-LMTO 27-atom supercell result; Le Bacq *et al.* (Ref. 11).
[f]Fully relaxed PP 54-atom supercell result; Satta *et al.* (Ref. 12).
[g]Fully relaxed PP 27-atom supercell result; Satta *et al.* (Ref. 13).

5% for all three metals, and we conclude that this behavior is generally true for all of the group-V bcc transition metals. From this result, one can also roughly estimate the magnitude of the structural relaxation energy measured from the unrelaxed configuration. In Ta, for example, the average force on an unrelaxed first-shell atom is about 0.32 eV/Å for a bond length of about 2.9 Å. The structural relaxation energy can then be computed as the work required to move the first-shell atoms to their relaxed positions,

$$\delta E^f_{vac} \sim -\frac{1}{2}\sum_{i=1}^{8} f_i \delta u_i , \tag{4}$$

where the sum is over the eight neighbors of the vacancy in the first-near-neighbor shell. With $f_i=0.32$ and $\delta u_i=2.9\times0.05$, we find the relaxation energy to be about 0.2 eV, which is close to what we obtain from our PP-LDA structural relaxations. Thus as a first approximation one can neglect second- and higher-neighbor shells in the relaxation of the vacancy in the group-V transition metals. The situation in the group-VI metals is qualitatively similar, except that the large 5% inward relaxation of the nearest-neighbor shell is reduced to an approximate 1% inward relaxation. Also, in Mo the second-neighbor shell also relaxes inward by about the same amount.

The relaxed geometries obtained from the PP calculations for V, Nb, Mo, Ta, and W were used in a second step to calculate fully relaxed LDA and GGA vacancy formation energies utilizing our all-electron FP-LMTO method. In practice, five volumes were calculated with the FP-LMTO approach for each metal using the relaxed PP geometry. This way volume relaxation was ensured for the applied PP configuration. For Cr and Fe, no PP calculations were attempted and, in lieu of these data, we instead used the relaxed configurations obtained from W and Ta, respectively. We believe this is reasonable because Cr and W are both group-V elements and Fe has a minority-spin *d*-band filling comparable to that of Ta.[28] As shown in Table V, the fully relaxed FP-LMTO-LDA results are generally in good agreement with the corresponding PP-LDA values, as are the FP-LMTO-GGA calculations. However, for the 3*d* metals, and Fe in particular, the GGA results are closer to experimental data than corresponding LDA calculations.

Our procedure using relaxed PP-LDA configurations as input into the computationally more expensive FP-LMTO calculations is an extremely efficient one because of the relative ease in relaxing structures with the plane-wave PP technique. Very recently, we have also been able to achieve direct structural relaxation with the FP-LMTO approach, albeit at a considerable penalty in computation effort (more than an order of magnitude). For two metals, Cr and Ta, this was actually carried through in detail for the LDA case as an additional check on our basic procedure outlined above. The values of E^f_{vac} so obtained for Cr and Ta are indeed in good agreement (less than 5% difference) with the results obtained using the PP-LDA configuration (Table V).

In comparing our volume-relaxed FP-LMTO-LDA results with those of Korhonen *et al.*,[7] we observe that our vacancy formation energies are close to theirs but somewhat larger in most metals, particularly in the case of W. Plane-wave PP calculations for W by Satta *et al.*[13] also gave a larger vacancy formation energy than that of Korhonen *et al.*, when done in a similar manner, i.e., with an unrelaxed 27-atom supercell. At the same time, the fully relaxed PP vacancy

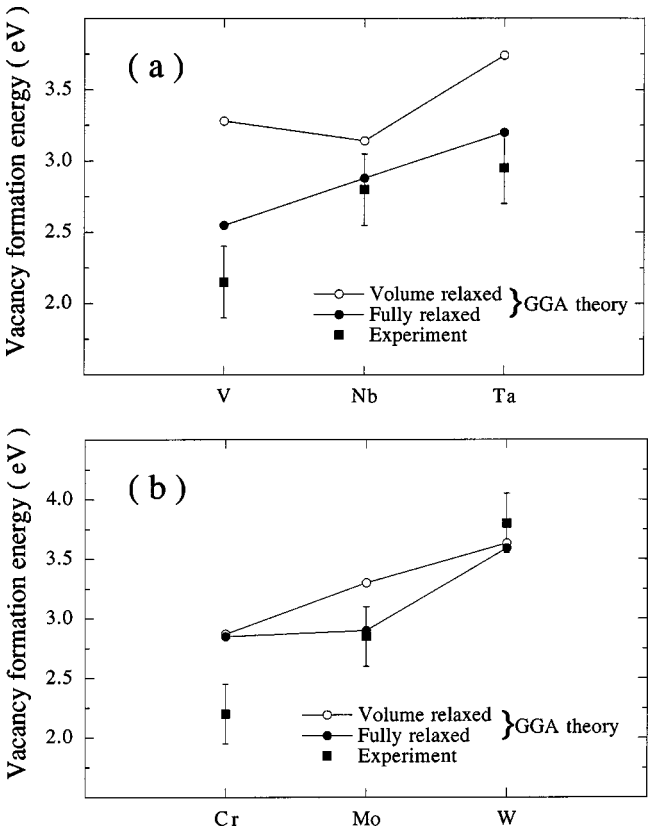

FIG. 2. Theoretical FP-LMTO-GGA calculations (open and filled circles) and experimental data (Refs. 23 and 24) (filled squares) for the vacancy formation energies in group-V (A) and group-VI (b) bcc *d*-transition metals. The error bars on the experimental data points are plotted ± 0.25 eV.

calculation on W by Satta *et al.*[13] is quite consistent with our FP-LMTO-LDA value, as shown in Table V. Satta *et al.* argues that the discrepancy between their results and the FP-LMTO result of Korhonen *et al.* was due to numerical approximations made in the FP-LMTO calculations. We propose instead that most of the discrepancy with Korhonen *et al.* for W is due to the lack of volume relaxation in their calculations. This can actually lead to a *smaller* vacancy formation energy in some cases, although this may seem somewhat counterintuitive. For Mo, we suggest that the result of Korhonen *et al.* was not well converged with respect to supercell size. We reproduced their vacancy formation energy within 2% when the calculations were done in a similar way (an unrelaxed 27-atom supercell).

In Fig. 2 we summarize our FP-LMTO-GGA results for the bcc metals in groups V [Fig. 2(a)] and VI [Fig. 2(b)]. Note that both the calculated and measured formation energies increase as one proceeds from the $3d$ metal to the $4d$ metal and to the $5d$ metal within a group, although the theoretical increase is less pronounced than the experimental trend. When we allow for structural relaxation in the calculations, all of the bcc metals except Cr are either within (Fe, Nb, Mo, Ta, or W) or close to (V) the error bars of experiment. As a point of reference for the Fe calculation, the vacancy formation energy for iron was recently calculated by Korzhavyi *et al.*[8] using their LMTO Green's-function method within the LDA, allowing for volume but not structural relaxation. They obtained a value of 2.25 eV, which should be compared to our LDA volume-relaxed value of 2.76 eV. Thus there is a real difference of about 0.5 eV. Moreover, as was suggested above, a good calculation of E^f_{vac} for iron implicitly requires the formation and accurate calculation of its magnetic moment. In this regard, our calculated magnetic moment per atom is close to $2.15\mu_B$ for all our iron calculations. This value is rather independent of either the presence of the vacancy or the choice of exchange-correlation treatment and is close to the reported bulk magnetic moment.[29]

IV. CONCLUSIONS

We have systematically studied vacancy formation energies for seven bcc *d*-transition metals from first-principles electronic structure methods, considering both LDA and GGA exchange-correlation treatments and allowing for both volume and structural relaxation in our calculations. While introduction of the GGA only substantially improves our results in the special case of Fe, the inclusion of full volume and structural relaxation lowers calculated values of E^f_{vac} from 0.1 to 0.5 eV, and universally improves agreement with experiment. The resulting overall agreement between theory and experiment is especially good for the $4d$ and $5d$ transition metals, whereas for the $3d$ metals the agreement is less impressive. In this regard, our fully relaxed FP-LMTO-LDA and GGA values of E^f_{vac} for the $4d$ and $5d$ bcc metals are all within the error bars of experimental data. Our fully relaxed FP-LMTO-GGA result for Fe is also within experimental error bars, but for V our best calculated PP-LDA value is about 0.3 eV above the largest experimental value. For Cr the situation is worse, with our lowest calculated E^f_{vac} (FP-LMTO-GGA) some 0.45 eV above the upper limit of experiment. At the same time, it should be noted that in both Fe and Cr there are remaining quantitative uncertainties due to the limited availability here of true fully relaxed geometries. For the LDA treatment of Cr, the use of a relaxed PP-LDA configuration from W was confirmed to be an adequate procedure by our directly relaxed FP-LMTO-LDA test calculations. For the GGA calculations on Fe and Cr, however, the use of relaxed PP-LDA configurations from W and Ta, respectively, is a more uncertain approximation. In the future, better fully relaxed calculations, using a direct FP-LMTO-GGA approach, would be desirable.

Previously, Korhonen *et al.*[7] speculated that use of the LDA was responsible for the discrepancies in V and Cr and that better approximations such as the GGA might improve the situation. Our study shows, however, that replacing the LDA with the GGA only slightly improves the agreement with experiment for these metals. In part, this may be related to the fact that we did not fully relax our structures using the GGA functional but instead used LDA configurations to calculate the final GGA total energies. With relaxed GGA geometries it is possible that our GGA calculations would have been in better agreement with experiment for V and Cr. On the other hand, for Fe the GGA did improve the vacancy formation energy considerably, especially when a relaxed LDA geometry was used. This was perhaps less surprising, however, since it is known that a GGA treatment correctly predicts the bcc ground state of iron, whereas use of the LDA fails to do so. As a whole, we have shown that LDA calcu-

lations, when performed carefully with volume and structural relaxations, give E^f_{vac} within experimental error bars for the bcc $4d$ and $5d$ transition metals. For these metals the GGA treatment results in similarly good agreement between theory and experiment. For the $3d$ metals V and Cr both LDA and GGA calculations overestimate E^f_{vac}, with the GGA treatment giving the better results. For Fe, GGA is necessary in order to obtain a realistic vacancy formation energy.

It should also be mentioned that recently the GGA was applied to calculate the unrelaxed vacancy formation energies in fcc Al, Cu, and Ni (Ref. 30) using a Green's-function Korringa-Kohn-Rostocker method. It was found that the GGA, in comparison to the LDA, lowered E^f_{vac} in these metals, although the differences were rather small and within the error bars of experimental data.

Finally, from our fully relaxed PP calculations, we conclude that first-shell relaxation around the vacancy is the most important structural effect and dominates the structural relaxation energy with the exception of Mo. For the cases studied here, the first shell relaxes inward toward the vacancy by about 5% for group-V transition metals and about 1% for group-VI metals. In the case of Mo, the second shell also relaxes inward by about 1%. The corresponding structural relaxation energies are consequently often significant. Except for Cr and W, where the value is on the order of 0.1 eV, the LDA structural relaxation energies are in the range 0.2–0.4 eV. This conclusion is in contradiction to the assumption made in recent theoretical studies[7,8] where this effect has been argued to be negligible. This may be true for fcc metals, which are more closely packed than the bcc metals, but it is certainly not true for the majority of the bcc transition metals.

ACKNOWLEDGMENTS

Valuable discussions with Dr. Phil Sterne and Dr. Chris Woodward are acknowledged. This work was performed under the auspices of the U.S. Department of Energy by the Lawrence Livermore National Laboratory under Contract No. W-7405-ENG-48.

[1] J. A. Moriarty, W. Xu, P. Söderlind, J. Belak, L. H. Yang, and J. Zhu, J. Eng. Mater. Technol. **121**, 120 (1999).
[2] P. Söderlind and J. A. Moriarty, Phys. Rev. B **57**, 10 340 (1998).
[3] P. Hohenberg and W. Kohn, Phys. Rev. **136**, B864 (1964).
[4] W. Kohn and L. J. Sham, Phys. Rev. **140**, A1133 (1965).
[5] B. Chakraborty, R. W. Siegel, and W. E. Pickett, Phys. Rev. B **24**, 5445 (1981).
[6] P. H. Dederichs, T. Hoshino, B. Drittler, K. Abraham, and R. Zeller, Physica B **172**, 203 (1991).
[7] T. Korhonen, M. J. Puska, and R. M. Nieminen, Phys. Rev. B **51**, 9526 (1995).
[8] P. A. Korzhavyi, I. A. Abrikosov, B. Johansson, A. V. Ruban, and H. L. Skriver, Phys. Rev. B **59**, 11 693 (1999).
[9] H. M. Polatoglu, M. Methfessel, and M. Scheffler, Phys. Rev. B **48**, 1877 (1993).
[10] B. Meyer and M. Fähnle, Phys. Rev. B **56**, 13 595 (1997).
[11] O. Le Bacq, F. Willaime, and A. Pasturel, Phys. Rev. B **59**, 8508 (1999).
[12] A. Satta, F. Willaime, and S. de Gironcolie, Phys. Rev. B **60**, 7001 (1999).
[13] A. Satta, F. Willaime, and S. de Gironcolie, Phys. Rev. B **57**, 11 184 (1998).
[14] U. von Barth and L. Hedin, J. Phys. C **5**, 1629 (1972).
[15] J. P. Perdew, J. A. Chevary, S. H. Vosko, K. A. Jackson, M. R. Pederson, and D. J. Singh, Phys. Rev. B **46**, 6671 (1992).
[16] J. M. Wills (unpublished); P. Söderlind, Ph.D thesis, Uppsala University, 1994; J. Trygg, Ph.D. thesis, Uppsala University, 1995; J. M. Wills and B. R. Cooper, Phys. Rev. B **36**, 3809 (1987); D. L. Price and D. R. Cooper, *ibid.* **39**, 4945 (1989).
[17] D. M. Ceperley and B. J. Alder, Phys. Rev. Lett. **45**, 566 (1980).
[18] J. P. Perdew and A. Zunger, Phys. Rev. B **23**, 5048 (1981).
[19] C. J. Wu, L. H. Yang, J. E. Klepeis, and C. Mailhiot, Phys. Rev. B **52**, 11 784 (1995).
[20] L. H. Yang, in *Industrial Strength Parallel Computing*, edited by A. Koniges (Morgan Kaufmann, San Francisco, 1999).
[21] O. H. Nielsen and R. M. Martin, Phys. Rev. Lett. **50**, 697 (1983).
[22] F. D. Murnaghan, Proc. Natl. Acad. Sci. USA **30**, 244 (1944).
[23] H. Schultz and P. Ehrhart, in *Atomic Defects in Metals*, edited by H. Ullmaier, Landolt-Börnstein, New Series, Group III, Vol. 25 (Springer, Berlin, 1991), p. 115.
[24] H.-E. Schaefer, Phys. Status Solidi A **102**, 47 (1987).
[25] K. Fürderer, K.-P. Döring, M. Gladisch, N. Hass, D. Herlach, J. Major, H.-J. Mundinger, J. Rosenkranz, W. Schäfer, L. Schimmele, M. Schmolz, W. Schwarz, and A. Seeger, in *Vacancies and Interstitials in Metals and Alloys*, edited by C. Abromeit and H. Wollenberger (Trans Tech, Switzerland, 1987), p. 125.
[26] L. De Schepper, G. Knuyt, L. M. Stals, D. Segers, L. Dorikens-Vanpraet, M. Dorikens, and P. Moser, in *Vacancies and Interstitials in Metals and Alloys* (Ref. 25), p. 131.
[27] R. Ziegler and H.-E. Schaefer, Mater. Sci. Forum **15–18**, 145 (1987).
[28] P. Söderlind, R. Ahuja, O. Eriksson, J. M. Wills, and B. Johansson, Phys. Rev. B **50**, 5918 (1994).
[29] M. B. Sterns in *Magnetic Properties of 3d, 4d, and 5d Elements, Alloys and Compounds*, edited by K.-H. Hellwege and O. Madelung, Landolt-Börnstein, New Series, Group III, Vol. 19, Pt. a (Springer, Berlin, 1984); D. Bonnenberg, K. A. Hempel, and H. P. J. Wijn, *ibid.*
[30] M. Asato, T. Hoshino, T. Asada, R. Zeller, and P. H. Dederichs, J. Magn. Magn. Mater. **177–181**, 1403 (1998).
[31] J. Donohue, *The Structure of the Elements* (Wiley, New York, 1974).
[32] C. Kittel, *Introduction to Solid State Physics*, 6th ed. (Wiley, New York, 1986).
[33] J. N. Mundy, Philos. Mag. A **46**, 345 (1982).